



DNA binding studies of a series of *cis*-[Pt(Am)₂X₂] complexes (Am = inert amine, X = labile carboxylato ligand)

Esther Escribano^a, Mercè Font-Bardia^{b,c}, Teresa Calvet^b, Julia Lorenzo^d, Patrick Gamez^{a,e}, Virtudes Moreno^{a,*}

^a Departament de Química Inorgànica, University of Barcelona, Martí i Franquès 1-11, 08028 Barcelona, Spain

^b Departament de Cristal·lografia, Mineralogia i Dipòsits Minerals, Martí i Franquès s/n, 08028 Barcelona, Spain

^c Centre Científic i Tecnològic de la Universitat de Barcelona (CCITUB), Unitat de Difracció de RX, Solé i Sabarís 1-3, 08028 Barcelona, Spain

^d Institut de Biotecnologia i Biomedicina, Universitat Autònoma de Barcelona, 08193 Bellaterra, Barcelona, Spain

^e Institució Catalana de Recerca i Estudis Avançats (ICREA), Passeig Lluís Companys, 23, 08010 Barcelona, Spain

ARTICLE INFO

Article history:

Received 7 May 2012

Received in revised form 16 July 2012

Accepted 17 July 2012

Available online 1 August 2012

Keywords:

Platinum dicarboxylate compounds

DNA binding

Atomic force microscopy

Platinum drugs

ABSTRACT

A series of platinum(II) complexes of formulae *cis*-[Pt(Am)₂X₂] (where Am represents an inert amine and X a labile (carboxylato) ligand) have been prepared and characterized by elemental analysis, ESI-MS, IR and ¹H NMR spectroscopy. The single-crystal molecular structures were determined for *cis*-[Pt(o-pea)(cbdca-2H)], *cis*-[Pt(hmpy)(cbdca-2H)], *cis*-[Pt(NH₃)₂(bzmal-2H)] and *cis*-[Pt(hmpy)(μ-dcch-2H)₂] (where **opea** is picolylamine, **hmpy** represents 4-hydroxymethylpyridine, **cbdca-2H**, is 1,1-cyclobutanedicarboxylate anion, **bzmal-2H** stands for benzylmalonate anion and **dcch-2H** is *trans*-1,2-cyclohexanedicarboxylate anion). The interaction of all compounds with DNA was investigated with different techniques: viscosity measurements and emission fluorescence spectroscopy were used to investigate the changes induced by the binding of the platinum compounds to calf-thymus DNA, while atomic force microscopy and electrophoretic mobility allowed evaluating the potential alterations of pBR322 plasmid DNA. The cytotoxic behavior of the platinum compounds on human leukemia HL-60 tumor cell lines was also examined.

© 2012 Elsevier B.V. All rights reserved.

1. Introduction

The anti-proliferative activity of *cis*-diamminedichloridoplatinum(II) (**cisplatin**; Fig. 1) was discovered serendipitously by Rosenberg and co-workers in 1965 [1]. A few years later, the anti-tumor activity of cisplatin was revealed [2], and in 1978 the US Food and Drug Administration (FDA) approved this compound for clinical use. Since then, this drug has been applied extensively in cancer chemotherapy, in the treatment of a number of solid tumors including genitourinary, colorectal, and non-small cell lung cancers [3–5]. Cisplatin is especially efficient against testicular cancer with a cure rate of over 90% and nearly 100% when tumors are diagnosed early [6]. However, the clinical use of cisplatin is restricted by several drawbacks. Serious potential side effects including nausea, vomiting, ototoxicity, neuropathy, myelosuppression and nephrotoxicity limit its usefulness [7–10]. In addition, many tumor cells display intrinsic or acquired resistance to platinum-based drugs, which further limits their practicality [11–13]. Hence, for over three decades, continuous research efforts have been dedicated to the development of improved platinum-based drugs to over-

come these limitations [14,15]. From the several thousand platinum compounds synthesized, only about 35 have entered clinical trials [16–18]. At present, besides cisplatin, two platinum drugs (**oxaliplatin**, **carboplatin**) are used clinically worldwide while **nedaplatin** was approved in Japan (Fig. 1) [11,19,20].

Most of the anticancer-active platinum coordination compounds exhibit the following general formula *cis*-[Pt(Am)₂X₂], Am being an inert amine and X a labile ligand (leaving group). For instance, *cis*-diammine(1,1-cyclobutanedicarboxylato)platinum(II) (carboplatin; Am = ammonia and X = 1,1-cyclobutanedicarboxylato) shows a mechanism of action that is comparable to that of cisplatin. However, carboplatin is less reactive than cisplatin [21].

Actually, the rate of aquation of the leaving group of carboplatin, namely the 1,1-cyclobutanedicarboxylato ligand, is nearly twice lower than that of cisplatin, owing to the chelating effect. Consequently, clinical treatment with carboplatin causes less severe side effects compared to cisplatin, even though higher doses are required [26]. Together with carboplatin, *cis*-diammine(glycolato)platinum(II) [27] (nedaplatin; Am = ammonia and X = glycolato) are members of the second-generation platinum drugs, for which the leaving groups X have been optimized to reduce the incidence of side effects. Both carboplatin and nedaplatin are cross-resistant to cisplatin, therefore indicating that their mecha-

* Corresponding author. Tel.: +34 93 4021274; fax: +34 93 4907725.

E-mail address: virtudes.moreno@qi.ub.es (V. Moreno).

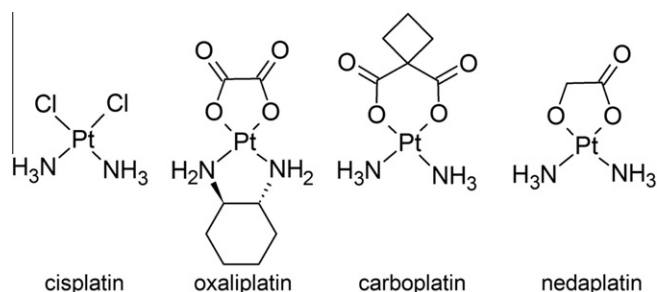


Fig. 1. Platinum(II) coordination compounds used in cancer chemotherapy: *cis*-diamminedichloridoplatinum(II) (**cisplatin**; [1]); [(1*R*,2*R*)-cyclohexane-1,2-diamine](oxalato)platinum(II) (**oxaliplatin**; [22,23]); *cis*-diammine(1,1-cyclobutanedicarboxylato)platinum(II) (**carboplatin**; [24]); *cis*-diammine(glycolato)platinum(II) (**nedaplatin**; [25]).

nisms of action are analogous. In the third-generation platinum drugs, the ammine ligands (Am = ammonia) are replaced by primary or secondary amine ligands. For example, in [(1*R*,2*R*)-cyclohexane-1,2-diamine](oxalato)platinum(II) [22] (oxaliplatin; Am = (1*R*,2*R*)-cyclohexane-1,2-diamine and X = oxalato), the NH₃ groups have been substituted with (1*R*,2*R*)-cyclohexane-1,2-diamine. Interestingly, the higher lipophilicity of the cyclohexanediamine ligand allows an enhanced uptake in cancer cells compared to cisplatin [28]. Thus, oxaliplatin displays a different spectrum of activity and is capable of circumventing cisplatin resistance [29], although the structure of its DNA adduct is similar to that of cisplatin [30,31].

In the present study, different families of *cis*-[Pt(Am)₂X₂] compounds have been developed, which combine a dicarboxylate ligand (as leaving group X) with distinct monoamine or diamine ligands (as inert Am ligands). Hence, 1,1-cyclobutanedicarboxylate (**cbdca-2H**), oxalate (**ox-2H**), *meso*-2,3-dibromosuccinate (**mdbs-2H**), *trans*-1,2-cyclohexanedicarboxylate (**dcch-2H**), benzylmalonate (**bzmal-2H**) have been used in combination with ammonia, 4-hydroxymethylpyridine (**hmpy**), ethylenediamine (**en**), tetramethylethylenediamine (**temed**), (1*R*,2*R*)-cyclohexane-1,2-diamine (**dach**), 2-picolyamine (**opa**) and 2-(2-pyridyl)ethylamine (**opea**) (Fig. 2). The preparation of such mixed X/Am Pt^{II} compounds is

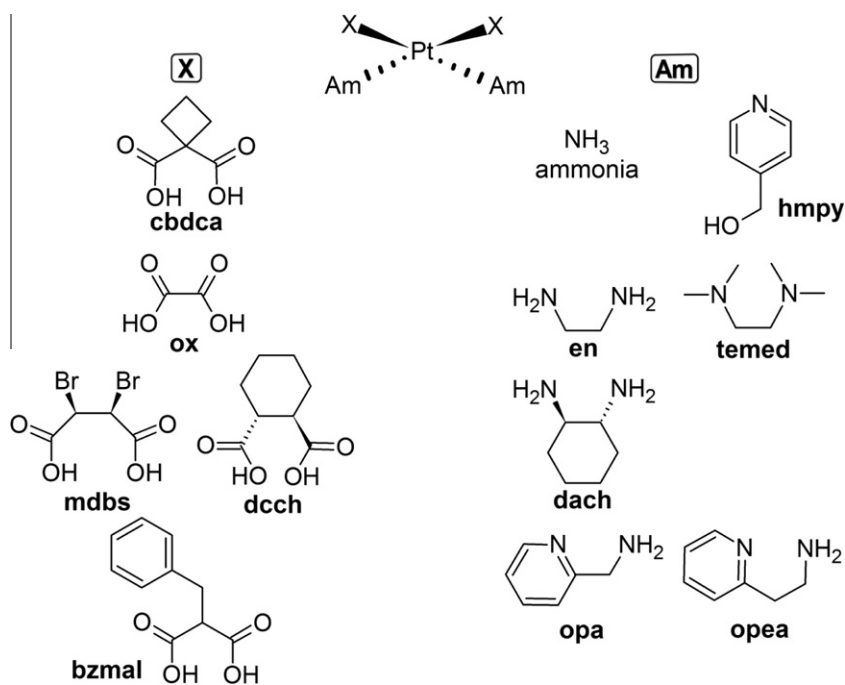


Fig. 2. Carboxylic acid (H₂X) and inert ligands (Am) used to prepare *cis*-[Pt(Am)₂X₂] compounds.

aimed at prospecting for new molecules with potential DNA-binding/cytotoxic properties.

The platinum(II) compounds obtained have been fully characterized and their DNA-interaction abilities have been studied by gel electrophoresis, viscosity and fluorescence measurements, atomic-force microscopy (AFM) and cytotoxicity assays.

2. Experimental

2.1. Materials and methods

Solvents and chemicals were commercially available as A.R. grade and used as received. All reactions and purifications were performed in air. Proton magnetic resonance (¹H NMR) spectra were recorded on a VARIAN UNITY (300 MHz) spectrometer at 25 °C. Proton chemical shifts are expressed in parts per million (ppm, δ scale) and are referenced to the solvent peak. Infrared spectra were recorded using a NICOLET-5700 FT-IR (in the range 4000–400 cm⁻¹), and data are represented as the frequency of absorption (cm⁻¹); the solid samples were prepared as KBr disks while liquids were deposited on a NaCl support. C, H, N analyses were carried out using an automatic Carlo Erba EA 1108 analyzer (analytical services of the Universitat de Barcelona). ESI Mass Spectroscopy was carried out using a LC/MSD-TOF Spectrometer from Agilent Technologies, equipped with an electrospray ionization (ESI) source (analytical services of the Universitat de Barcelona). The melting points or decomposition temperatures of the compounds were determined with a Stuart Scientific SMP3 apparatus, using a capillary.

2.2. Preparation of platinum(II) coordination compounds

All *cis*-[Pt(Am)₂X₂] compounds described in the present study have been obtained using Dhara's method [32], as follows:



440.7 mg of K₂[PtCl₄] (1.06 mmol) were dissolved in 15.6 mL of distilled water at 35 °C, under an inert atmosphere of nitrogen. 1.08 g of KI (6.5 mmol) were dissolved in 1.5 mL of distilled water.

The resulting aqueous solution of potassium iodide was added to the red solution of potassium tetrachloridoplatinate. The resulting dark-green mixture was stirred for 20 min before utilization in the next synthetic step.

cis – [Pt(Am)₂I₂]

In a three-necked round-bottomed flask of 100 mL equipped with two dropping funnels and a Liebig condenser were introduced 13.4 mL of distilled water. A solution of 1.08 mmol of the amine Am in 17.8 mL of distilled water was introduced in one of the two dropping funnels. The second dropping funnel contained 1.08 mmol of K₂[PtCl₄] in 17.8 mL of distilled water. After purging with nitrogen, the flask was warmed to 60 °C and the two solutions were simultaneously and slowly added under stirring to the round-bottomed flask (during a period of approx. 60 min). A yellow precipitate appeared during the addition of the two reactants. The reaction mixture was subsequently cooled down slowly to room temperature, and the solid material was isolated by filtration on a glass filter, and washed with ethanol (2 × 5 mL) and diethyl ether (6 mL). The yellow solid obtained was stored in a desiccator.

Ag₂X

An aqueous solution of 2 mmol of NaOH (or NaHCO₃ in the case of *meso*-2,3-dibromosuccinate; **mdbs-2H**) was added to 1 mmol of de dicarboxylic acid (H₂X) dissolved in the minimum of distilled water. The mixture was kept in the dark, and 2 mmol of silver(I) nitrate were added which yielded a white precipitate. The heterogeneous mixture was stirred for 15–30 min and the silver salt, i.e. Ag₂X, was isolated by filtration and stored in a desiccator.

cis – [Pt(Am)₂X]

A one-to-one mixture of *cis*-[Pt(Am)₂I₂] and Ag₂X in 15 mL of distilled water was stirred in the dark during 2–3 days. The resulting precipitate, i.e. AgI, was removed by filtration over Celite and the subsequent filtrate was concentrated to dryness using a rotary evaporator. The solid obtained, namely *cis*-[Pt(Am)₂X] was washed with cold distilled water and diethyl ether.

2.2.1. ethylenediamine(1,1-cyclobutanedicarboxylato)platinum(II), [Pt(en)cbdc] (1)

This compound was earlier described by Rochon and co-workers [33]. View supporting info.

2.2.2. N,N,N',N'-tetramethylethylenediamine(1,1-cyclobutanedicarboxylato)platinum(II), [Pt(temed)(cbdc-2H)] (2)

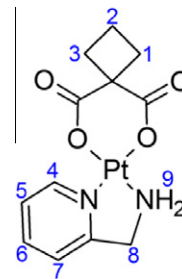
This compound was before reported by Rochon and co-workers [34]. View supporting info.

2.2.3. (Trans-1,2-cyclohexanediamine)(1,1-cyclobutanedicarboxylato)platinum(II), [Pt(dach)(cbdc-2H)] (3)

This compound was before synthesized by Pierpont and co-workers [35]. View supporting info.

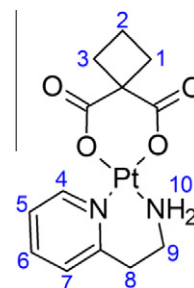
2.2.4. (2-(Aminomethyl)pyridine)(1,1-cyclobutanedicarboxylato)platinum(II), [Pt(opa)(cbdc-2H)] (4)

Yield = 22%. Mw = 445.33 g mol⁻¹. ¹H NMR (D₂O, 300 MHz, 25 °C): δ 1.75 (2, m, 2H, ³J = 8 Hz), δ 2.29 (3, t, 2H, ³J = 8 Hz), δ 2.72 (1, t, 2H, ¹J = 8 Hz), δ 4.13 (8, s, 2H), δ 7.28 (5, t, 1H, ³J = 6.6 Hz), δ 7.39 (7, d, 1H, ³J = 8 Hz), δ 7.92 (6, t, 1H, ³J = 8 Hz), δ 8.23 (4, d, 1H, d, ³J = 6 Hz) ppm. IR (KBr pellet, cm⁻¹): ν = 3450–3200 (NH₂), 1635 (C = O + NH₂ + C = N). ESI-MS (*m/z*, positive mode): ([M+H]⁺) 446, ([M+Na]⁺) 468, ([2 M+Na]⁺) 914. Anal. Calc. for (%) for PtN₂H₁₄C₁₂O₄·1.5H₂O: C, 30.51; H, 3.63; N, 5.93. Found: C, 31.12; H, 3.27; N, 6.21%. Compound **4** is partially soluble in water, soluble in DMF and methanol, but not in chloroform.



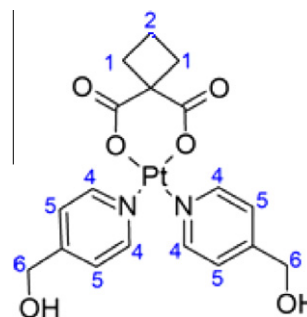
2.2.5. (2-(Aminoethyl)pyridine)(1,1-cyclobutanedicarboxylato)platinum(II), [Pt(opea)(cbdc-2H)] (5)

Yield = 36%. Mw = 459.36 g mol⁻¹. ¹H NMR (D₂O, 300 MHz, 25 °C): δ 1.78 (2, m, 2H, ³J = 8 Hz), δ 2.39 (9, t, 2H, ³J = 5 Hz), δ 2.77 (1 and 3, t, 4H, ³J = 8 Hz), δ 3.03 (8, t, 2H, ³J = 5 Hz), δ 7.27 (5, t, 1H, ³J = 6.8 Hz), δ 7.36 (7, d, 1H, ³J = 8 Hz), δ 7.86 (6, dd, 1H, ³J = 8 Hz), δ 8.44 (4, d, 1H, ³J = 6.5 Hz) ppm. IR (KBr pellet, cm⁻¹): ν = 3200 (NH₂), 1640 and 1615 (C = O + NH₂ + C = N), 1371 (C–O). ESI-MS (*m/z*, positive mode): ([M+H]⁺) 460, ([M+Na]⁺) 482, ([2 M+Na]⁺) 942, ([2 M+H]⁺) 920. Anal. Calc. for (%) for PtN₂H₁₆C₁₃O₄·2H₂O: C, 31.52; H, 4.07; N, 5.65. Found: C, 31.62; H, 3.87; N, 5.52%. Compound **5** is partially soluble in water and chloroform, and soluble in DMSO, DMF and methanol. The molecular structure of **5** could be determined by single-crystal X-ray diffraction (see text and SI for details).



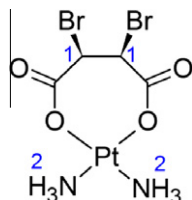
2.2.6. Bis-(4-pyridinemethanol)(1,1-cyclobutanedicarboxylato)platinum(II), [Pt(hmpy)₂(cbdc-2H)] (6)

Yield = 59%. Mw = 555.45 g mol⁻¹. ¹H NMR (D₂O, 300 MHz, 25 °C): δ 1.87 (2, m, 1H, ³J = 7.8 Hz), δ 2.90 (1, t, 4H, ³J = 8.0 Hz), δ 4.60 (6, s, 4H, overlapped with the solvent), δ 7.37 (5, d, 4H, ³J = 5.7 Hz), δ 8.40 (4, d, 4H, ³J = 5.7 Hz) ppm. IR (KBr pellet, cm⁻¹): ν = 1648 (C = O), 1619 (C = N), 1368 (C–O), 476 (Pt–N). ESI-MS (*m/z*, positive mode): ([M+H]⁺) 556, ([M+Na]⁺) 578, ([2 M+Na]⁺) 1134, ([2 M+H]⁺) 1112. Anal. Calc. for (%) for PtN₂H₂₀C₁₈O₆·1.5H₂O: C, 38.92; H, 3.63; N, 5.04. Found: C, 37.09; H, 3.65; N, 4.39%. Compound **6** decomposes above 168 °C. **6** is soluble in water, DMSO and DMF, and not soluble in chloroform and methanol. The molecular structure of **6** could be determined by single-crystal X-ray diffraction (see text and SI for details).



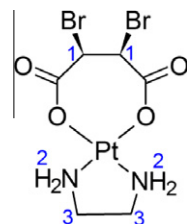
2.2.7. Diammine(meso-2,3-dibromosuccinato)platinum(II), [Pt(NH₃)₂(mdbS-2H)] (**7**)

Yield = 27%. Mw = 503.01 g mol⁻¹. ¹H NMR (D₂O, 300 MHz, 25 °C): δ 3.99–4.14 (2, br, 6H), δ 4.44 (1, s, 2H) ppm. IR (KBr pellet, cm⁻¹): ν = 3202 (NH), 1684 (C=O + NH₂). ESI-MS (*m/z*, positive mode): ([M+H]⁺) 504, ([M+Na]⁺) 526. Anal. Calc. for (%) for PtN₂H₈C₄O₄Br₂: C, 9.55; H, 1.60; N, 5.57. Found: C, 9.58; H, 1.82; N, 5.58%. Compound **7** decomposes above 193 °C. **7** is soluble in water and DMSO, and not soluble in chloroform, DMF and methanol.



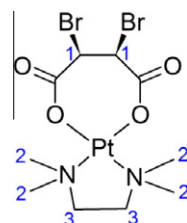
2.2.8. Ethylenediamine(meso-2,3-dibromosuccinato)platinum(II), [Pt(en)(mdbS-2H)] (**8**)

Yield = 24%. Mw = 529.04 g mol⁻¹. ¹H NMR (D₂O, 300 MHz, 25 °C): δ 2.53 (s, 4H), δ 4.39 (s, 2H), δ 5.13 (br, 4H) ppm. IR (KBr pellet, cm⁻¹): ν = 3240 (NH₂), 1719 (C=O), 1617 (NH₂), 1052 (C–O), 540 (Pt–N). ESI-MS (*m/z*, positive mode): ([M+H]⁺/2) 265. Anal. Calc. for (%) for PtN₂H₁₀C₄O₄Br₂: C, 13.60; H, 2.09; N, 5.29. Found: C, 13.26; H, 2.04; N, 6.12%. Compound **8** decomposes above 152 °C. **8** is soluble in water, DMSO and DMF, and not soluble in chloroform and methanol.



2.2.9. N,N,N',N'-tetramethylethylenediamine(meso-2,3-dibromosuccinato)platinum(II), [Pt(temed)(mdbS-2H)] (**9**)

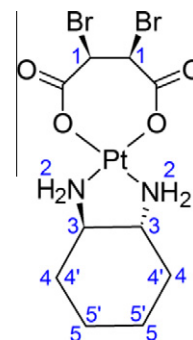
Yield = 56%. Mw = 585.15 g mol⁻¹. ¹H NMR (D₂O, 300 MHz, 25 °C): δ 2.32 (12H, br), δ 2.75 (4H, br), δ 4.34 (2H, br) ppm. IR (KBr pellet, cm⁻¹): ν = 1734 and 1653 (C=O), 1341 (C–O), 548 (Pt–N). ESI-MS (*m/z*, positive mode): ([M+H]⁺) 586, ([M–Br]⁺) 505, ([M+Na]⁺) 608, ([M+NH₄]⁺) 603. Anal. Calc. for (%) for PtN₂H₁₈C₁₀O₄Br₂: C, 20.53; H, 3.10; N, 4.79. Found: C, 20.39; H, 3.09; N, 4.71%. Compound **9** decomposes above 147 °C. **9** is partially soluble in water, soluble in DMSO and DMF, and not soluble in chloroform and methanol.



2.2.10. (Trans-1,2-cyclohexanediamine)(meso-2,3-dibromosuccinato)platinum(II), [Pt(dach)(mdbS-2H)] (**10**)

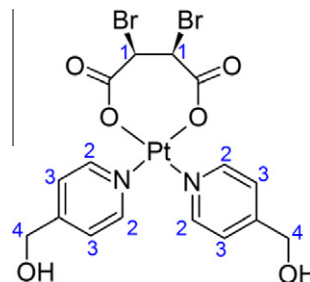
Yield = 8%. Mw = 583.14 g mol⁻¹. ¹H NMR (D₂O, 300 MHz, 25 °C): δ 1.06 (5, br, 2H), δ 1.21 (4, br, 2H), δ 1.49 (5', br, 2H), δ 1.96 (4', br, 2H), δ 2.33 (3, br, 2H), δ 4.38 (1, s, 2H) ppm. IR (KBr pellet, cm⁻¹): ν = 3253 (NH₂), 1719 (C=O), 1617 (NH₂), 1065 (C–O).

ESI-MS (*m/z*, positive mode): ([M+H]⁺) 584. Anal. Calc. for (%) for PtN₂H₁₆C₁₀O₄Br₂: C, 20.60; H, 2.77; N, 4.80. Found: C, 21.33; H, 2.89; N, 4.92%. Compound **10** decomposes above 170 °C. **10** is partially soluble in water, soluble in DMSO and DMF, and not soluble in chloroform and methanol.



2.2.11. Bis-(4-pyridinemethanol)(meso-2,3-dibromosuccinato)platinum(II), [Pt(hmpy)₂(mdbS-2H)] (**11**)

Yield = 89.5%. Mw = 687.20 g mol⁻¹. ¹H NMR (D₂O, 300 MHz, 25 °C): δ 4.37 (1, s, 2H), δ 4.62 (4, s, 4H), δ 7.33 (3, br, 4H), δ 8.53 (2, br, 4H) ppm. IR (KBr pellet, cm⁻¹): ν = 1622 (C=O + C=N), 1053 (C–O), 807 (C–H), 491 (Pt–N). ESI-MS (*m/z*, positive mode): ([M+H]⁺) 688, ([M+Na]⁺) 710. Anal. Calc. for (%) for PtN₂H₁₆C₁₆O₆Br₂·3H₂O: C, 25.93; H, 2.99; N, 3.78. Found: C, 25.56; H, 2.92; N, 4.32%. Compound **11** decomposes above 142 °C. **11** is partially soluble in water, soluble in DMSO and DMF, and not soluble in chloroform and methanol.



2.2.12. Diammine(benzylmalonato)platinum(II), [Pt(NH₃)₂(bzma-2H)] (**12**)

This compound was earlier described by Ye et al. [36]. View supporting info.

2.2.13. Ethylenediamine(benzylmalonato)platinum(II), [Pt(en)(bzmal-2H)] (**13**)

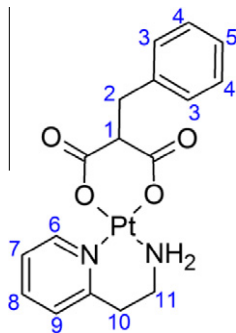
This compound was earlier described by Rochon and co-workers [33]. View Supporting info.

2.2.14. N,N,N',N'-tetramethylethylenediamine(benzylmalonato)platinum(II), [Pt(temed)(bzma-2H)] (**14**)

Yield = 28.5%. Mw = 503.46 g mol⁻¹. ¹H NMR (D₂O, 300 MHz, 25 °C): δ 2.75 (7, s, 12H), δ 2.79 (6, s, 4H), δ 3.68 (2, d, 2H, ³J = 10 Hz), δ 3.78 (1, t, 1H ³J = 10 Hz), δ 7.26–7.37 (3, 4, 5, 5H) ppm. IR (KBr pellet, cm⁻¹): ν = 1640 (C=O), 1380 (C=O). ESI-MS (*m/z*, positive mode): ([M+H]⁺) 504, ([M+Na]⁺) 526, ([2M+H]⁺) 1008, ([2M+Na]⁺) 1030. Anal. Calc. for (%) for PtN₂H₂₄C₁₆O₄: C, 38.17; H, 4.80; N, 5.56. Found: C, 37.51; H, 4.56; N, 5.54%. Compound **14** decomposes above 82.5 °C. **14** is partially soluble in water and methanol, soluble in DMSO and DMF, and not soluble in chloroform.

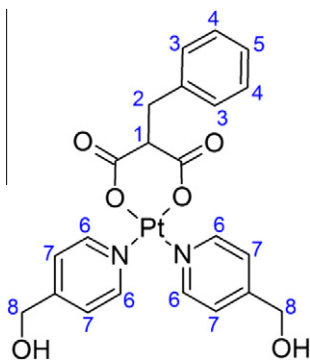
2.2.15. (2-(Aminoethyl)pyridine)(benzylmalonato)platinum(II), [Pt(oepa)(bzmal-2H)] (**15**)

Yield = 6%. Mw = 485.40 g mol⁻¹. ¹H NMR (D₂O, 300 MHz, 25 °C): δ 2.56 (11, br, 2H), δ 2.73 (10, br, 2H), δ 3.16 (2, br, 2H), δ 3.32 (1, br, 1H), δ 7.13–7.23 (3, 4, 5, br, 5H), δ 7.36 (7, t, 1H, ³J = 8 Hz), δ 7.55 (9, d, 1H, ³J = 8 Hz), δ 7.85 (8, t, 1H, ³J = 9 Hz), δ 8.78 (6, d, 1H, ³J = 8 Hz) ppm. IR (KBr pellet, cm⁻¹): ν = 3235 (NH), 1636 and 1617 (C=O + NH₂ + C=N), 1384 (C=O). ESI-MS (*m/z*, positive mode): ([M+H]⁺) 486, ([2 M+H]⁺) 973. Anal. Calc. for (%) for PtN₂H₂₄C₁₆O₄: C, 37.12; H, 3.74; N, 5.77. Found: C, 36.68; H, 3.62; N, 5.03%. Compound **15** is partially soluble in water, soluble in DMSO and DMF, and not soluble in chloroform and methanol.



2.2.16. Bis-(4-pyridinemethanol)(benzylmalonato)platinum(II), [Pt(hmpy)₂(bzmal-2H)] (**16**)

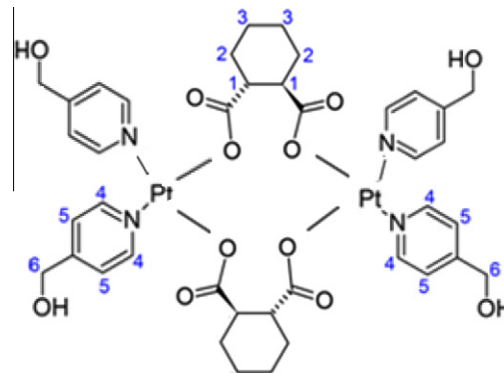
Yield = 75%. Mw = 605.51 g mol⁻¹. ¹H NMR (D₂O, 300 MHz, 25 °C): δ 2.92 (2, d, 2H, ³J = 8 Hz), δ 3.27 (1, t, 1H, ³J = 8 Hz), δ 7.19–7.26 (3, 4, 5, br, 5H), δ 8.18 (7, br, 4H), δ 8.37 (6, br, 4H) ppm. IR (KBr pellet, cm⁻¹): ν = 1656 and 1629 (C=O), 1384.5 (C=O), 1054 (C–O). ESI-MS (*m/z*, positive mode): ([M+H]⁺) 606, ([M+Na]⁺) 628, ([2 M+H]⁺) 1212, ([2 M+Na]⁺) 1234. Anal. Calc. for (%) for PtN₂H₂₂C₂₂O₆: C, 43.64; H, 3.66; N, 4.63. Found: C, 43.07; H, 3.12; N, 4.11%. Compound **16** decomposes above 184 °C. **16** is partially soluble in water, soluble in DMSO and DMF, and not soluble in chloroform and methanol.



2.2.17. Tetrakis-(4-pyridinemethane)-bis-(μ-trans-1,2-cyclohexanedicarboxylato)diplatinum(II), [Pt₂(hmpy)₄(μ-dcch-2H)₂] (**17**)

Yield = 83%. Mw = 583.50 g mol⁻¹. ¹H NMR (D₂O, 300 MHz, 25 °C): δ 4.59 (6, s, 4H), δ 7.26 (5, 4H), δ 8.35 (4, 4H) ppm. The hydrogens H¹, H² and H³ are not well resolved. IR (KBr pellet, cm⁻¹): ν = 1622 (C=O + C=N), 1059 (C–O), 497 (Pt–N). ESI-MS (*m/z*, positive mode): ([M+H]⁺) 584, ([2 M+H]⁺) 1168, ([2 M+Na]⁺) 1190. Anal. Calc. for (%) for Pt₂N₄H₄₈C₄₀O₁₂: C, 41.17; H, 4.15; N, 4.80. Found: C, 40.24; H, 4.31; N, 4.69%. Compound **17** decomposes above 210.5 °C. **17** is partially soluble in DMF, soluble in water, DMSO and methanol, and not soluble in chloroform. The molecular

structure of **17** could be determined by single-crystal X-ray diffraction (see text and SI for details).



2.3. Gel electrophoresis of platinum-pBR322 complexes

The stock solutions of the platinum(II) compounds were prepared as above in TE containing 2% DMSO. pBR322 plasmid DNA aliquots (0.25 μg/mL) were incubated in TE (Tris-H₄edta, Tris(hydroxymethyl)aminomethaneethylenediaminetetracetic acid) buffer (50 mM NaCl, 10 mM Tris.HCl, 1 mM H₄edta, pH = 7.5) at molar ratio *r*_i = 0.50 for electrophoresis study. Incubation was carried out at 37 °C for 24 h. The charge (4 μL) marker were added to 20 μL aliquot parts of the compound-DNA adduct. The resulting mixture was electrophoretized on agarose gel (0.5% in TBE buffer, Tris-Borate-EDTA) for 4 h at 1.5 V/cm. Subsequently, the DNA was dyed with an ethidium bromide solution (0.5 μg/mL in TBE) for 20 min. Samples of free DNA and of cisplatin-DNA complex were used as controls. The experiment was carried out in an ECO-GEN horizontal tank connected to a PHARMACIA GPS 200/400 variable potential power supply and the gel was photographed with a thermal imager FUJIFILM FTI-500.

2.4. Atomic force microscopy (TMAFM)

pBR322 DNA was stirred gently at room temperature for 15 min to obtain a homogeneous distribution of DNA topoisomers. Pt complex stock solutions (1 mg/mL) were prepared freshly in 40 mM HEPES buffer ((HEPES = *N*-2-hydroxyethyl piperazine-*N'*-2-ethanesulfonic acid), 10 mM MgCl₂, pH = 7.4) containing 2% DMSO. These solutions were diluted 1000 times with HEPES to give 2000 μL of the Pt solutions. Each sample was prepared by addition of 1 μL of pBR322 DNA (0.25 μg/μL) to 2 μL of complex stock solution, and the final volume was adjusted to 50 μL with HEPES. The different solutions as well as Milli-Q water were passed through 0.2 nm FP030/3 filters (Scheicher & Schuell GmbH, Germany) to provide a clear background when they were imaged by AFM. All samples were incubated at 37 °C for 24 h. The AFM samples were prepared by casting a 2-μL drop of test solution onto freshly cleaved Muscovite green mica disks as the support. The drop was allowed to stand undisturbed for 3 min to favor the adsorbate/substrate interaction. Each DNA-laden disk was rinsed with Milli-Q water and was blown dry with clean compressed argon gas directed normal to the disk surface. The samples were stored over silica prior to AFM imaging. All Atomic Force Microscopy (AFM) observations were made with a Nanoscope III Multimode AFM (Digital Instrumentals, Santa Barbara, CA). Nano-crystalline Si cantilevers of 125-nm length with a spring constant of 50 N/m average ended with conical-shaped Si probe tips of 10-nm apical radius and cone angle of 35° were utilized. High-resolution topographic AFM images were obtained in air at room temperature (relative humidity <40%) on different

specimen areas of $2 \times 2 \mu\text{m}$ operating in intermittent contact mode at a rate of 1–3 Hz.

2.5. Viscosity measurements

The viscosity experiments were carried out at a constant temperature of 25 °C with an AND-SV-1 viscometer in a water bath using a water jacket accessory. A range of 20–100 μL of 10 mM solutions (in TE containing 2% DMSO) of the different platinum compounds were added to 2 mL of a 100 mM ct-DNA solution in TE. The flow time was measured by a digital stop watch. Kinetic studies were performed over a time period of 24 h.

2.6. Fluorescence measurements

A 50 μM solution of *Calf Thymus* DNA (ct-DNA) in a TE buffer solution was prepared. 30 μL of a 5 mM solution of ethidium bromide were added to 3 mL aliquots of the ct-DNA solution. The resulting mixtures were incubated at 37 °C for 30 min or 24 h. Next, 20, 40, 60, 80 and 100 μL of Pt complex solutions (containing no more than 2% DMSO) were added to the 3 mL aliquots, giving concentrations of 10, 20, 30, 40 and 50 μM , respectively. Each Pt compound of the present study was investigated with incubation times of 30 min and 24 h. The emission spectra were recorded in the range 530–670 nm, with an excitation wavelength of 502 nm. The fluorescence measurements were performed with a KONTRON SFM 25 spectrofluorometer.

2.7. Growth-inhibition assays

2.7.1. Tumor cell lines and culture conditions

The cell line used for the cytotoxic tests was the human acute promyelocytic leukemia cell line HL-60 (American Type Culture Collection (ATCC)). The cells were routinely maintained in RPMI-1640 medium supplemented with 10% (v/v) heat inactivated fetal bovine serum, 2 mM glutamine, 100 U/mL penicillin, and 100 $\mu\text{g}/\text{mL}$ streptomycin (Gibco BRL, Invitrogen Corporation, Netherlands) in a highly humidified atmosphere of 95% air with 5% CO_2 at 37 °C.

2.7.2. Cytotoxicity assays

The potential growth-inhibitory effect of the platinum complexes on the leukemia HL-60 cell line was estimated using the MTT assay [37]. Cells growing in the logarithmic phase were seeded in 96-well plates (10^4 cells per well), and subsequently treated with varying doses of the platinum complexes and the reference drug, i.e. cisplatin, at 37 °C for 24 or 72 h. For each of the variations tested, four wells were used. Aliquots (20 μL) of a MTT solution were then added to each well. After 3 h, the colored formazan formed was quantified by a spectrophotometric plate reader at 490 nm wavelength. The percentage of cell viability was calculated by dividing the average absorbance of the cells treated with the complex by that of the control; IC_{50} values (drug concentration at which 50% of the cells are viable relative to the control) were obtained using the GraphPad Prism software, version 4.0. Each experiment was repeated at least three times, and each concentration tested in at least six replicates.

3. Results and discussion

3.1. Syntheses of the platinum(II) coordination compounds

A series of seventeen $[\text{Pt}(\text{Am})_2\text{X}_2]$ complexes have been prepared through the combination of various inert **Am** ligands and labile **X** ligands (see Fig. 2), applying Dhara's synthetic procedure (see Section 2) [32]. The compounds obtained are listed in Table 1.

Table 1

$[\text{Pt}(\text{Am})_2\text{X}_2]$ compounds prepared from inert ligands (**Am**) and Labile ligands (**X**) depicted in Fig. 2.

X ligand	Am ligand	Pt compound
cbdca-2H	NH₃	carboplatin
ox-2H	dach	oxaliplatin
cbdca-2H	en	<i>cis</i> -[Pt(en)(cbdca-2H)] (1)
cbdca-2H	temed	<i>cis</i> -[Pt(temed)(cbdca-2H)] (2)
cbdca-2H	dach	<i>cis</i> -[Pt(dach)(cbdca-2H)] (3)
cbdca-2H	opa	<i>cis</i> -[Pt(opa)(cbdca-2H)] (4)
cbdca-2H	opea	<i>cis</i> -[Pt(opea)(cbdca-2H)] (5)
cbdca-2H	hmpy	<i>cis</i> -[Pt(hmpy) ₂ (cbdca-2H)] (6)
mdbs-2H	NH₃	<i>cis</i> -[Pt(NH₃) ₂ (mdbs-2H)] (7)
mdbs-2H	en	<i>cis</i> -[Pt(en)(mdbs-2H)] (8)
mdbs-2H	temed	<i>cis</i> -[Pt(temed)(mdbs-2H)] (9)
mdbs-2H	dach	<i>cis</i> -[Pt(dach)(mdbs-2H)] (10)
mdbs-2H	hmpy	<i>cis</i> -[Pt(hmpy) ₂ (mdbs-2H)] (11)
bzmal-2H	NH₃	<i>cis</i> -[Pt(NH₃) ₂ (bzmal-2H)] (12)
bzmal-2H	en	<i>cis</i> -[Pt(en)(bzmal-2H)] (13)
bzmal-2H	temed	<i>cis</i> -[Pt(temed)(bzmal-2H)] (14)
bzmal-2H	opea	<i>cis</i> -[Pt(opea)(bzmal-2H)] (15)
bzmal-2H	hmpy	<i>cis</i> -[Pt(hmpy) ₂ (bzmal-2H)] (16)
dccp-2H	hmpy	[Pt ₂ (hmpy) ₄ (μ - dccp-2H) ₂] (17)

3.2. Single crystal X-ray diffraction

The molecular structures of compounds **5**, **6**, **12** and **17** have been determined by single-crystal X-ray diffraction (see SI for the X-ray crystallographic analysis and data collection). Selected bond lengths and angles for these coordination compounds are given as Supporting information.

3.2.1. Crystal structure of $\{[\text{Pt}(\text{opea})(\text{cbdca-2H})]_2(\text{H}_2\text{O})_3\}$ (**5**)₂·3H₂O

The two-day reaction of $[\text{Pt}(\text{opea})\text{I}_2]$ with $\text{Ag}_2(\text{cbdca-2H})$ in water yields, after filtration of the AgI salt produced, single crystals of (**5**)₂·3H₂O after two months. (**5**)₂·3H₂O crystallizes in the monoclinic space group $P2_1/c$ (Table S1). The single-crystal X-ray structure of (**5**)₂ is depicted in Fig. 3.

The unit cell contains two mononuclear Pt^{II} molecules that are almost identical (Fig. S1 and Table S2). Therefore, only one of them will be described in detail. The metal center Pt1 is tetracoordinated by one **cbdca-2H** ligand (carboxylato oxygen atoms O11 and O13) and one **opea** ligand (pyridine nitrogen atom N11 and amino nitrogen atom N12), generating a nearly perfect square plane (the angles vary from 88.3(3) to 92.0(3)°; Table S2). The Pt–N and Pt–O bond distances are in normal range for this type of coordination environment [38,39]. The cyclobutyl ring of **cbdca-2H** is perpendicular to the platinum square plane, as is observed for carboplatin [40].

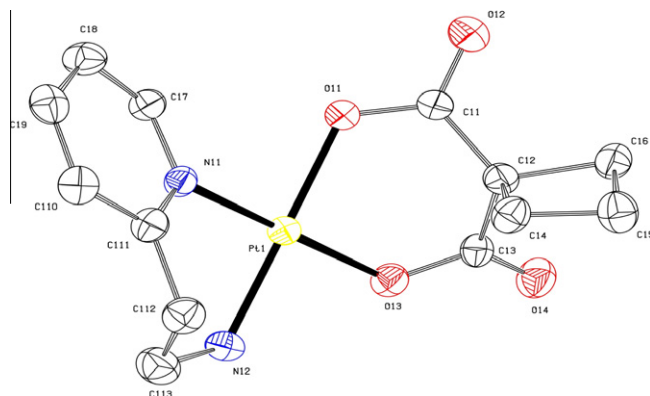


Fig. 3. Representation of the molecular structure of $[\text{Pt}(\text{opea})(\text{cbdca-2H})]$ (**5**). Hydrogen atoms and lattice water molecules are omitted for clarity. Only one of the two slightly different *cis*-platinum(II) molecules present in the unit cell is shown (see Fig. S1).

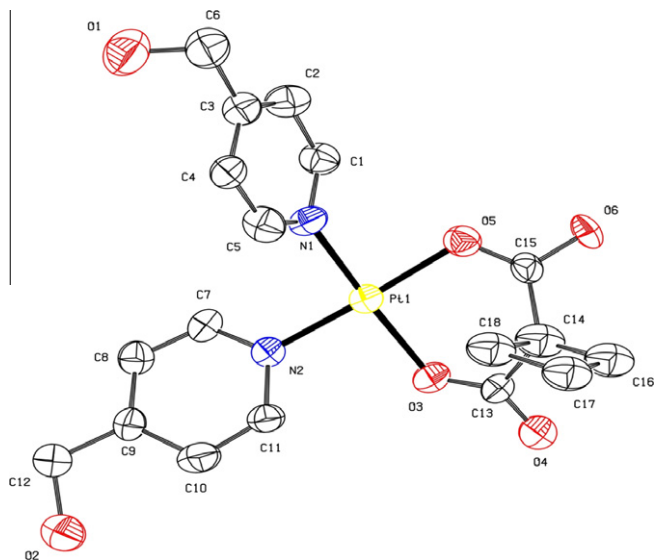


Fig. 4. Representation of the molecular structure of $[Pt(\text{hmpy})_2(\text{cbdca-2H})]$ (**6**). Hydrogen atoms are omitted for clarity.

The crystal structure of (**5**) $_2 \cdot 3\text{H}_2\text{O}$ exhibits an intricate intermolecular network of O–H...O and N–H...O bonds involving lattice water molecules and the amino and carboxylato groups of the platinum units. Hence, eight molecules of **5** are arranged around eleven water molecules. This supramolecular organization results in the formation of 1D channels that are filled with water molecules (Fig. S2).

3.2.2. Crystal structure of $[Pt(\text{hmpy})_2(\text{cbdca-2H})]$ (**6**)

The reaction of $[Pt(\text{hmpy})_2\text{I}_2]$ with $\text{Ag}_2(\text{cbdca-2H})$ in water solution yields, after filtration of the AgI salt produced, single crystals of compounds **6** after a two months period. Single-crystal X-ray studies revealed that **6** crystallizes in the monoclinic space group $P2_1/c$. A perspective view of the molecular structure of **6** is represented in Fig. 4.

Details for the structure solution and refinement are summarized in Table S3, and selected bond distances and angles are listed in Table S4. The molecule is a mononuclear platinum(II) compound consisting of a tetracoordinated metallic center in a square-planar coordination environment (Fig. 4). The square plane is formed by the carboxylato oxygen atoms O3 and O5 belonging to one bidentate **cbdca-2H** ligand, and two pyridine nitrogen atoms (N1 and N2) from two monodentate **hmpy** ligands. The almost perfect square-planar geometry is characterized by coordination angles ranging from 87.9(3) to 92.1(3) $^\circ$ (Table S4). The bond lengths and angles are in normal ranges for this type of coordination compounds [38,41].

The crystal structure of **6** exhibits an intricate intermolecular network of O–H...O bonds, which connects the alcoholic O–H group of the **hmpy** ligand to two neighboring platinum molecules, resulting in a supramolecular 3D framework (Fig. S3).

3.2.3. Crystal structure of $[Pt(\text{NH}_3)_2(\text{bzmal-2H})]$ (**12**)

The reaction of $[Pt(\text{NH}_3)_2\text{I}_2]$ with $\text{Ag}_2(\text{bzmal-2H})$ in water gave single crystals of **12** after two months. **12** crystallizes in the monoclinic space group Pc (Table S5). The single-crystal X-ray structure of **12** is depicted in Fig. 5.

Selected bond distances and angles are listed in Table S6. The platinum(II) ion of the mononuclear compound is tetracoordinated by two ammine ligands (nitrogen atoms N11 and N12) and two oxygen atoms (O11 and O13) belonging to one carboxylato

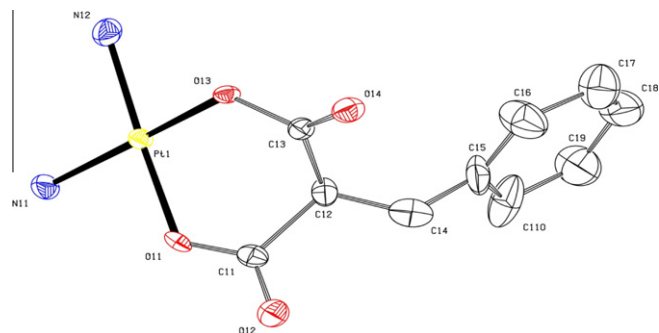


Fig. 5. Representation of the molecular structure of $[Pt(\text{NH}_3)_2(\text{bzmal-2H})]$ (**12**). Hydrogen atoms are omitted for clarity.

bzmal-2H ligand. The resulting slightly distorted square plane is characterized by coordination angles varying from 83.9(8) to 97.2(9) $^\circ$. The N11–Pt–N12 angle of 97.2(9) $^\circ$ reflects the repulsion between the ammine ligands, which is a feature that has been observed for related platinum complexes [42,43]. As a result, all other coordination angles of the square plane are below 90 $^\circ$. The Pt–N and Pt–O bond distances are in normal ranges for such coordination compounds [33].

In addition, the crystal structure of **12** exhibits a remarkable network of supramolecular interactions. Molecules of **12** are hydrogen-bonded to each other via N–H...O contacts, which generate a 1D chain (Fig. S4; green dotted lines). Two 1D chains intermingle through π – π interactions between the phenyl rings of the **bzmal-2H** ligands (Fig. S4; red dotted lines) that give rise to the formation of a zipper-like architecture. The ammine ligands and the carboxylato H-acceptor groups are further involved in H-bonding contacts, which produce a 3D supramolecular framework (Fig. S5).

3.2.4. Crystal structure of $[Pt_2(\text{hmpy})_4(\mu\text{-dcch-2H})_2]$ (**17**)

The reaction between $[Pt(\text{hmpy})_2\text{I}_2]$ and $\text{Ag}_2(\text{dcch-2H})$ in water solution for 24 h yielded, after filtration of the AgI salt produced, single crystals of **17**·2H₂O after several months. Single-crystal X-ray studies revealed that **17**·2H₂O crystallizes in the orthorhombic space group $Pbcn$. A perspective view of the molecular structure of **17** is represented in Fig. 6.

Details for the structure solution and refinement are summarized in Table S7, and selected bond distances and angles are listed in Table S8. The molecule is a dinuclear platinum(II) compound consisting of tetracoordinated metallic centers in a square-planar coordination environment. The square planes (for Pt1 and Pt1a) are formed by two nitrogen atoms belonging to two **hmpy** ligands and two carboxylato oxygen atoms from two different **dcch-2H** ligands, which are connecting the two platinum atoms through a double bridge (Fig. 6). The Pt–N and Pt–O bond lengths are comparable to those of compounds previously reported in the literature that exhibit similar environment features [44,45]. The coordination angles, varying from 86.92(19) to 92.51(18) $^\circ$, illustrate a slight distortion of the square-planar coordination geometry, which is most likely due to some steric constraints arising from the bridging binding mode of the **dcch-2H** ligand. The angle between the coordination plane of the platinum dimer is 23.30 $^\circ$.

The crystal structure of **17**·2H₂O exhibits an intricate intermolecular network involving C–OH...O_{C=O}, OH_{water}...O_{C=O} and C–OH...O_{water} hydrogen bonds (Fig. S6). Hence, each molecule of **17** is connected to four neighbors via C–OH...O_{C=O} contacts (Fig. S6A), and to two other adjacent molecules of **17** through four water molecules, by means of OH_{water}...O_{C=O} and C–OH...O_{water} bonds (Fig. S6B). This supramolecular organization of the dinuclear

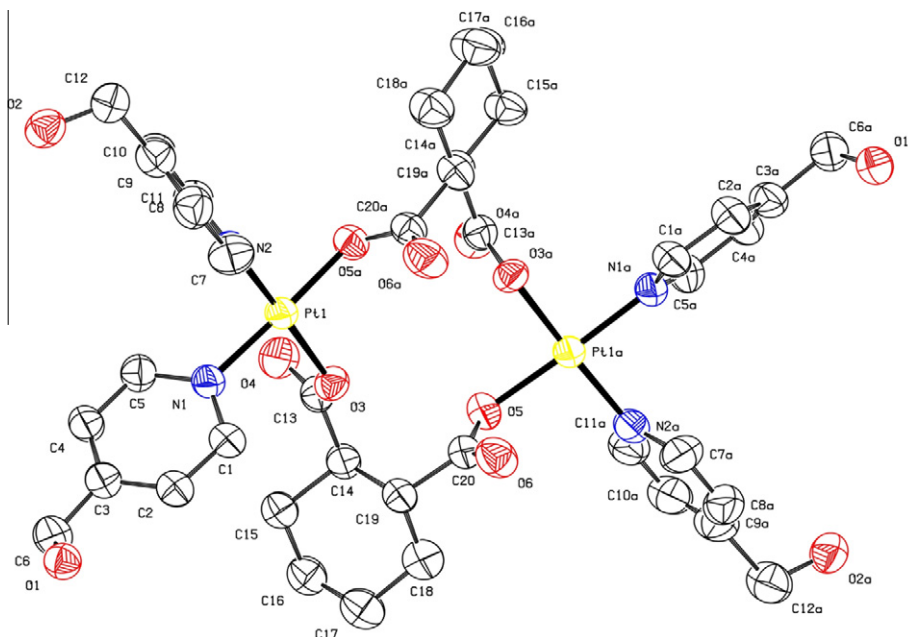


Fig. 6. Representation of the molecular structure of $[\text{Pt}_2(\text{hmpy})_4(\mu\text{-dcch-2H})_2]$ (**17**). Hydrogen atoms and lattice water molecules have been omitted for clarity. Symmetry operation: $a = -x, y, -z + 1/2$.

platinum(II) compounds in the lattice gives rise to a 3D framework (Fig. S6C).

3.3. Tapping mode atomic force microscopy (TMAFM)

Direct visualization of three conformers of plasmid DNA can be achieved using tapping mode atomic force microscopy (TMAFM) and thus allows graphically evaluating the interaction of plasmid DNA with for instance platinum coordination compounds. The AFM images of pBR322 plasmid DNA incubated with the platinum compounds of the series $[\text{Pt}(\text{Am})_2(\text{cbda-2H})]$ (complexes **1–6**; Table 1) are depicted in Fig. 7 and the corresponding to cisplatin,

carboplatin and oxaliplatin and to the complexes **7–17** in Figs. S7–S10.

Compound **1** generates a number of crossing points and DNA supercoiling is clearly observed (Fig. 7A). This modification of the morphology of the plasmid DNA is indicative of a strong interaction of **1** with pBR322 [46]. The AFM image illustrating the formation of **2**-DNA adducts is depicted in Fig. 7B. Supercoiled forms of DNA are present in small quantity, and some crossing points are detected; hence, compound **2** does not show strong interaction with DNA. A comparable behavior is observed for compound **4** (Fig. 7D). In contrast, compound **3** exhibits a distinct compartment. A significant aggregation of DNA is noticed (Fig. 7C), which results

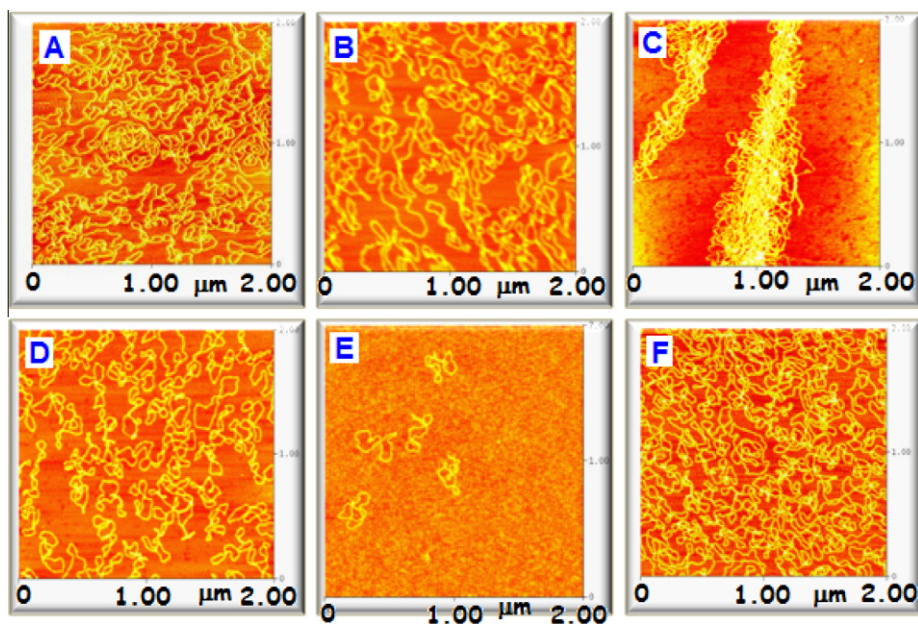


Fig. 7. TMAFM images of pBR322 plasmid DNA incubated at 37 °C for 24 h with A) $[\text{Pt}(\text{en})(\text{cbda-2H})]$ (**1**), B) $[\text{Pt}(\text{tmed})(\text{cbda-2H})]$ (**2**), C) $[\text{Pt}(\text{dach})(\text{cbda-2H})]$ (**3**), D) $[\text{Pt}(\text{opa})(\text{cbda-2H})]$ (**4**), E) $[\text{Pt}(\text{opea})(\text{cbda-2H})]$ (**5**) and F) $[\text{Pt}(\text{hmpy})_2(\text{cbda-2H})]$ (**6**).

from the abundant Pt-mediated crossing points that produce supercoiled forms, in high percentage. Compound **5** does not notably modify the morphology of pBR322 plasmid DNA, and mainly relaxed forms (OC) are present (Fig. 7E). Similarly, compound **6** does not seem to affect the morphology of DNA, therefore suggesting poor interaction between this complex and DNA (Fig. 7F).

From the series of compounds **7–11**, the compound **8** is the platinum(II) complex that affects most the DNA strands (Fig. S8B). Compound **7** modifies the morphology of pBR322 DNA, and CCC forms are predominantly seen in the corresponding picture (Fig. S8A). The aggregation of the forms observed for compound **9**, in Fig. S8C, may be due to the presence of a water layer over the mica surface. Complex **11** does not seem to modify significantly the morphology of pBR322 plasmid DNA.

The AFM images of pBR322 plasmid DNA incubated with the platinum compounds of the series [Pt(Am)₂(bzm₂H)] (complexes **12–16**; Table 1) are depicted in Figs. S9 and S10. The interaction between compound **12** and DNA results in broken DNA strands, as a consequence of severe tensions caused by the coordination of the platinum complex. Compound **15** induces clear alterations of the DNA structure, with crossing points, kinks and broken strands with microfolds (Fig. S9D). The AFM image of pBR322 plasmid DNA incubated with the platinum(II) complex [Pt₂(hmpy)₄(μ-dcch-2H)₂] (complex **17**; Table 1) is depicted in Fig. S10. This figure clearly evidences that **17** does not affect notably the tertiary structure of DNA.

3.4. Electrophoretic mobility

The influence of compounds **1–17** on the tertiary structure of DNA was investigated further by their ability to modify the electrophoretic mobility of the covalently closed circular (CCC) and open (OC) forms of pBR322 plasmid DNA. The results are shown in Figs. 8–10. In the pattern corresponding to the pBR322 plasmid DNA (Fig. 8, lanes 1 and 15; Fig. 9, lane 1 and Fig. 10, lane 1) a clear difference between the OC and CCC bands is noticed. In lanes 2 of Figs. 8–10 and lane 14 of Fig. 8, the typical coalescence of the two bands resulting from the action of cisplatin is evident.

For compounds **1–17**, the electrophoresis data largely complement those obtained from the AFM studies (see above).

Compounds **2, 5–7, 9, 11, 13–17** do not affect the DNA mobility on the agarose gel and it has been observed by AFM that these Pt^{II} complexes do not notably modify the morphology of pBR322 plasmid DNA (see Figs. S8–S10). For compounds **3, 4** and **10** (Fig. 8), the CCC and OC bands start to merge, therefore indicating an alteration of the DNA mobility.

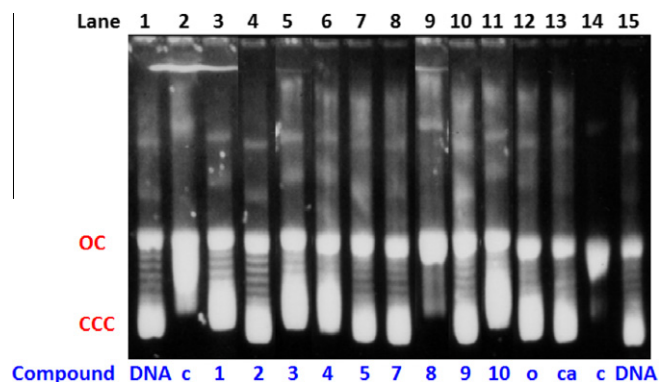


Fig. 8. Agarose gel electrophoretic mobility of DNA pBR322 (lanes 1 and 15) and treated with cisplatin (c, lane 2); compound **1** (lane 3); compound **2** (lane 4); compound **3** (lane 5); compound **4** (lane 6); compound **5** (lane 7); compound **7** (lane 8); compound **8** (lane 9); compound **9** (lane 10); compound **10** (lane 11); oxaliplatin (o, lane 12); carboplatin (ca, lane 13) and cisplatin (c, lane 14).

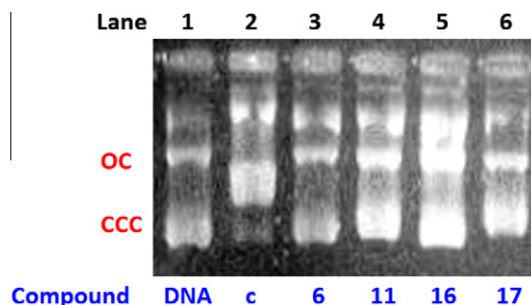


Fig. 9. Agarose gel electrophoretic mobility of DNA pBR322 (lane 1) and treated with cisplatin (c, lane 2); compound **6** (lane 3); compound **11** (lane 4); compound **16** (lane 5) and compound **17** (lane 6).

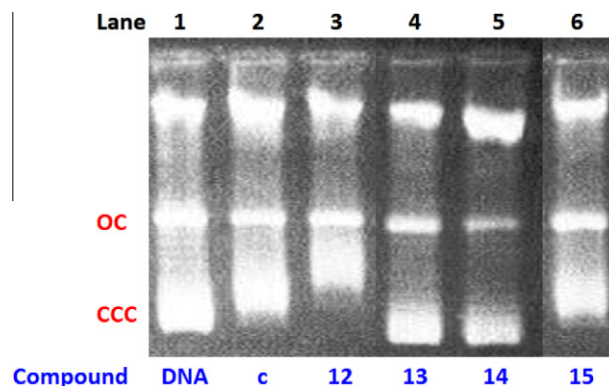


Fig. 10. Agarose gel electrophoretic mobility of DNA pBR322 (lane 1) and treated with cisplatin (c, lane 2); compound **12** (lane 3); compound **13** (lane 4); compound **14** (lane 5) and compound **15** (lane 6).

Actually, slight modifications of the tertiary structure of pBR322 plasmid DNA have been noted by AFM for these complexes. Compound **8**, similarly to cisplatin, induces the complete coalescence of the CCC and OC bands. The formation of OC forms has been observed by AFM (Fig. S8B). Finally, compound **12** clearly affects the DNA electrophoretic mobility, since the CCC form is not detected (Fig. 10). Interestingly, AFM studies have revealed the presence of broken DNA strands with **12** (Fig. S9A). In summary, it appears that [Pt(en)(mdbs-2H)] (**8**) and [Pt(NH₃)₂(bzm₂H)] (**12**) exhibit the strongest interaction with DNA.

3.5. Viscosimetry measurements

The potential interaction between the platinum(II) complexes and DNA was examined further by viscosimetry measurements. Such studies give information about the possible way(s) the coordination compounds interact with the DNA helix. Hence, the intercalation of the metal compound will induce a length change since base pairs will have to separate to accommodate the binding of the ligand; this will result in an increase in DNA viscosity [47]. In contrast, partial or non-intercalation may lead to a bend (or kink) of the DNA helix, giving rise to a diminution of its effective length and therefore its viscosity [48].

The values of relative specific viscosity (η/η_0)^{1/3} versus the molecular ratio, i.e. r_i , in the absence and in the presence of the complexes (**1**)–(**6**) are plotted in Fig. 11.

For carboplatin (Fig. 11), the viscosity decreases with increasing r_i , thus suggesting conformational changes of *ct*-DNA, due to the coordination of the platinum moiety. Compound **1** induces an abrupt decrease of the viscosity at $r_i = 0.1$, which is ascribed to

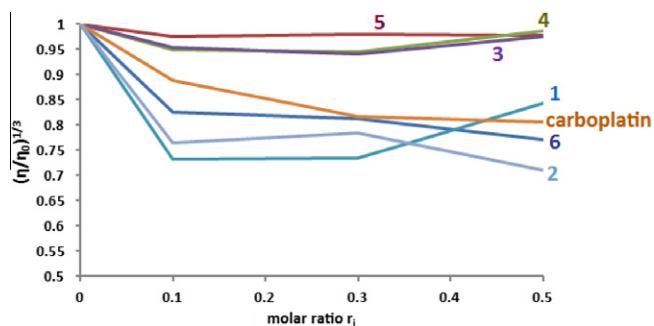


Fig. 11. Viscosimetry data, at $r_i = 0.1, 0.3$ and 0.5 , for carboplatin and the coordination compounds [Pt(en)(cbdca-2H)] (**1**), [Pt(temed)(cbdca-2H)] (**2**), [Pt(dach)(cbdca-2H)] (**3**), [Pt(opa)(cbdca-2H)] (**4**), [Pt(opea)(cbdca-2H)] (**5**) and [Pt(hmpy)₂(cbdca-2H)] (**6**).

the formation of *cis*-bifunctional DNA intrastrand adducts that leads to a bend of the DNA molecule, lessening its viscosity. At $r_i = 0.5$ $(\eta/\eta_0)^{1/3}$ increases (Fig. 11), which may be explained by the aggregation of DNA molecules (as observed by AFM; see above and Fig. 7A) that results in an increase of viscosity. At $r_i = 0.1$ and 0.3 , compound **2** exhibits a behavior similar to that of **1**; however, at $r_i = 0.5$ $(\eta/\eta_0)^{1/3}$ still decreases, therefore suggesting that the ligand temed (contrary to en) does not allow DNA aggregation (Fig. 11). The compartment of complexes **3** and **4** is related to that of **1**, albeit their effect on the conformational changes is minor (compared to that of **1**). Compound **5** does not appear to significantly affect the structure of the *ct*-DNA helix (Fig. 11). The slight decrease noticed may be attributed to the weak binding of the complex through hydrogen bonds, for instance with the phosphate backbone. Lastly, the binding between compound **6** and *ct*-DNA shows characteristics that are comparable to those of **2** (Fig. 11), which most likely arise from the formation of interstrand adducts that causes a conformational change, from the B-form to the Z-form.

Compounds **7**, **9** and **10** (Fig. S11, Supporting information) present $(\eta/\eta_0)^{1/3}$ versus r_i trends that resemble those of compounds **2** and **6** (Fig. 11). Most likely, these complexes bind DNA covalently via the nitrogen N7 of guanine, producing a local opening of double helix that reduces the viscosity. Compound **8** (Fig. S11) shows the major effects in this series. The clear diminution of the viscosity at $r_i = 0.1$ is probably due to the creation of interstrand adducts that modifies the DNA conformation. The subsequent increase of the viscosity, from $r_i = 0.1$ to $r_i = 0.3$ may be an indication of groove binding (surface binding) at higher loading of complex [47]. Finally, at very high complex loading, namely at $r_i = 0.5$ $(\eta/\eta_0)^{1/3}$

decreases, thus suggesting that this compound experiences competitive DNA interactions through covalent or groove binding. Compound **11** (Fig. S11) displays behavior similar to that of **5**, hence implying that this complex interacts with DNA mostly through H bonds.

The values of relative specific viscosity $(\eta/\eta_0)^{1/3}$ versus r_i for the series *cis*-[Pt(Am)₂(bzmal-2H)] (complexes **12–16**; Table S5) are plotted in Fig. S12, Supporting information.

Compounds **12** and **13** show similar behaviors, that is a decrease of the viscosity up to $r_i = 0.3$, followed by an increase at $r_i = 0.5$. The diminution of $(\eta/\eta_0)^{1/3}$ may be ascribed to the formation of interstrand adducts that alter the secondary structure of DNA. The subsequent increase of viscosity is most likely due to groove binding, by means of hydrogen-bonding contacts involving the N–H groups. The $(\eta/\eta_0)^{1/3}$ versus r_i trend for [Pt(temed)(bzmal-2H)] (**14**) (Fig. S12) is related to those of [Pt(temed)(cbdca-2H)] (**2**) (Fig. 11) and [Pt(en)(mdbs-2H)] (**8**) (Fig. S11). Hence, a significant decrease of viscosity is detected at $r_i = 0.1$, which may be explained by the bend (or kink) of the DNA helix induced by the creation of *cis*-bifunctional intrastrand DNA-complex adducts. The successive increase (at $r_i = 0.3$) and decrease of the viscosity (at $r_i = 0.5$) are indicative of the occurrence of different types of interactions between the Pt moiety and the DNA molecule, apparently due to the potential ability of the complexes to generate both hydrogen bonds (groove binding) and/or covalent bonds. The $(\eta/\eta_0)^{1/3}$ versus r_i values for compounds **15** and **16** do not indicate any major conformational changes. Actually, ligands that bind exclusively in the DNA grooves (like netropsin or distamycin), under the same conditions, typically cause less pronounced changes (positive or negative) or no changes in DNA solution viscosity. Therefore, these results suggest that **15** and **16** are mostly groove binders.

For [Pt₂(hmpy)₄(μ-dcch-2H)₂] (**17**), a slight diminution of the viscosity is noticed up to $r_i = 0.3$ (Fig. S13), which is ensued by a minor growth at $r_i = 0.5$. Again, this behavior is indicative of non-covalent binding to DNA through hydrogen-bonding contacts (with the phosphate backbone) or/and π - π stacking interactions (between bases).

3.6. Competitive binding studies using fluorescence spectroscopy

Ethidium bromide (EtBr), a cationic dye that can interact with DNA through intercalation is used commonly in spectroscopic studies [49–52]. Upon binding to DNA, EtBr shows characteristic changes in absorbance, reflected by an enhancement in

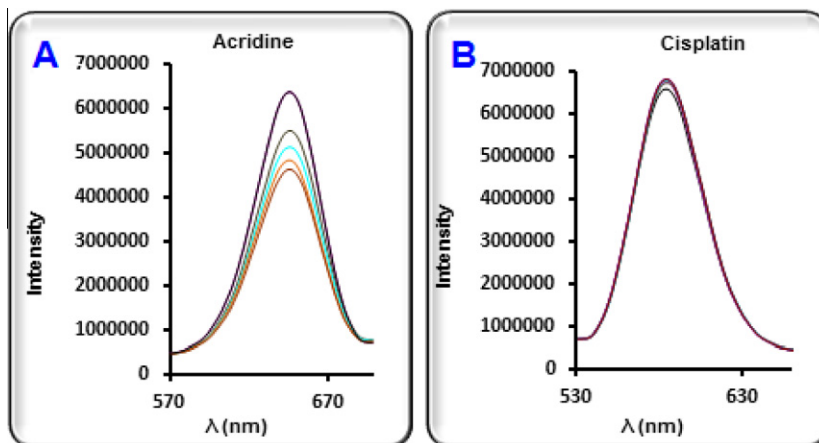


Fig. 12. Emission spectra of the EtBr–DNA complex (EtBr stands for ethidium bromide) in the presence of increasing concentrations of (A) acridine and (B) cisplatin, at room temperature, after an incubation time of 30 min.

fluorescence intensity by about one order of magnitude, as compared to free dye in solution [53].

Hence, when a platinum compound is added to the EtBr–DNA complex, any quenching of the fluorescence will indicate the replacement of EtBr by the coordination molecule, by intercalation.

Fig. 12 illustrate the competitive binding between EtBr and Acridine or cisplatin. Acridine is better intercalator than EtBr; therefore, its addition gives rise to a release of EtBr in the solution associated with a diminution of the emission (Fig. S15A). In contrast, cisplatin cannot displace EtBr, which is indicated by the absence of fluorescence quenching (Fig. S15B).

Competitive binding studies have been carried out for compounds **3**, **4**, **5**, **6**, **8**, **11**, **12**, **15**, **16** and **17**, and the corresponding emission spectra (recorded after incubation times of 30 min and 24 h) are depicted in Figs. S14–S23 (Supporting information). The compounds have been selected on the basis of the results obtained with other characterization techniques (described above) or to clarify the outcome of the viscosimetry measurements (see previous section). As is clearly evidenced in Figs. S11–S20, the Pt^{II} compounds investigated do not induce a significant quenching of the fluorescence resulting from the release of EtBr, thus suggesting that they cannot displace the cationic dye and efficiently intercalate into DNA. These fluorescence studies thus suggest that all the platinum(II) compounds reported herein are not effective DNA intercalators. Consequently, the interactions observed using other characterization techniques indicate that they occur via different mechanisms (such as covalent or hydrogen bonding).

3.7. Cytotoxic activity

The potential cytotoxicity of the platinum complexes **1–11** and cisplatin (for comparison) on human leukemia cancer cells (HL-60) was examined using the MTT assay, a colorimetric determination of cell viability during *in vitro* treatment with a drug. Compounds **12–17** could not be assayed due to their insolubility under the experimental conditions used. The assay, developed as an initial stage of drug screening, measures the amount of MTT reduction by mitochondrial dehydrogenase and assumes that cell viability (corresponding to the reductive activity) is proportional to the production of purple formazan that is measured spectrophotometrically. Low IC₅₀ values will be indicative of cytotoxicity or antiproliferation at low drug concentrations. Cells were incubated with each compound for a period of 72 h, and were assayed subsequently for growth using the MTT endpoint assay. The IC₅₀ values characterizing the growth inhibition of HL-60 cells induced by complexes **1–11** and cisplatin are summarized in Table 2. Most platinum complexes presented herein exhibit poor cytotoxic properties against HL-60 cells; therefore, apoptosis studies were not performed. The best IC₅₀ value, i.e. 9.53 ± 3.01 μM, was obtained

Table 2
IC₅₀ (μM) against tumor cell Line HL-60 values for cisplatin and complexes **1–11**.

Complex	72 h
cisplatin	2.15 ± 0.1
1	>200
2	>200
3	9.53 ± 3.01
4	79.72 ± 5.61
5	>200
6	70.66 ± 6.82
7	68.52 ± 4.37
8	>150
9	59.82 ± 8.33
10	60.71 ± 6.41
11	61.83 ± 4.37

after an incubation time of 72 h for [Pt(dach)(cbdca-2H)] (**3**), the corresponding value for cisplatin (control) being 2.15 ± 0.1 μM, under the same experimental conditions.

4. Conclusions

A series of platinum(II) complexes have been synthesized and the molecular structures of four of them have been determined by X-ray diffraction studies. The interaction between DNA and the coordination compounds have been appraised using different techniques, namely viscosity measurements, emission fluorescence spectroscopy and atomic force microscopy (AFM), which show that indeed they bind to the biological macromolecule. For instance, the AFM images of samples of the compounds incubated with plasmid pBR322 DNA reveal very strong DNA/compound interactions of different types, attributed predominantly to supercoiling, stacking and fragmentation. Surprising, only one of the complexes prepared, namely [Pt(dach)(cbdca-2H)] (**3**), presents an interesting IC₅₀ value, in the same order of magnitude as that of cisplatin. Compound **3** contains the inert amine (*trans*-cyclohexanediamine; **dach**) found in oxaliplatin and the labile dicarboxylate ligand (1-cyclobutanedicarboxylate; **cbdca-2H**) present in carboplatin. These results clearly demonstrate the difficulty to obtain potential platinum-based anti-cancer agents, even through the combination of ligands that have generated efficient systems (depicted in Fig. 1). The lack of cytotoxicity exhibited by most of the compounds may be explained by difficulties in the internalization processes into the cells or a more inert character of the carboxylate ligands compared to its chloride counterparts.

Acknowledgments

Financial support from the Spanish Ministry of Ciencia e Innovación, Contracts CTQ2008-02064 and BIO2010-22321-C02-01 are kindly acknowledged. Esther Escribano thanks the University of Barcelona for granting her a Ph.D. scholarship.

Appendix A. Supplementary material

CCDC 865068–865071 contains the supplementary crystallographic data for this paper. These data can be obtained free of charge from The Cambridge Crystallographic Data Centre via www.ccdc.cam.ac.uk/data_request/cif. Supplementary data associated with this article can be found, in the online version, at <http://dx.doi.org/10.1016/j.ica.2012.07.018>.

References

- [1] B. Rosenberg, L. Vancamp, T. Krigas, *Nature* 205 (1965) 698.
- [2] B. Rosenberg, L. Vancamp, J.E. Trosko, V.H. Mansour, *Nature* 222 (1969) 385.
- [3] T. Boulikas, M. Vougiouka, *Oncol. Rep.* 11 (2004) 559.
- [4] G. Giaccone, *Drugs* 59 (2000) 9.
- [5] B.A. Chabner, T.G. Roberts, *Nat. Rev. Cancer* 5 (2005) 65.
- [6] G.J. Bosl, D.F. Bajorin, J. Sheinfeld, R. Motzer, *Cancer of the testis*, Lippincott Williams & Wilkins, Philadelphia, PA, 2001.
- [7] P. Pil, S.J. Lippard, in: J.R. Bertino (Ed.), *Encyclopedia of Cancer*, Academic Press, San Diego, CA, 1997.
- [8] J. Reedijk, *Chem. Commun.* (1996) 801.
- [9] L.P. Rybak, C.A. Whitworth, D. Mukherjee, V. Rarakumar, *Hear. Res.* 226 (2007) 157.
- [10] F.E. de Jongh, R.N. van Veen, S.J. Veltman, R. de Wit, M.E.L. van der Burg, M.J. van den Bent, A.S.T. Planting, W.J. Graveland, G. Stoter, J. Verweij, *Br. J. Cancer* 88 (2003) 1199.
- [11] M.A. Fuertes, C. Alonso, J.M. Perez, *Chem. Rev.* 103 (2003) 645.
- [12] M. Kartalou, J.M. Essigmann, *Mutat. Res.-Fundam. Mol. Mech. Mutagen.* 478 (2001) 23.
- [13] C.A. Rabik, M.E. Dolan, *Cancer Treat. Rev.* 33 (2007) 9.
- [14] M.C. Ackley, C.G. Barry, A.M. Mounce, M.C. Farmer, B.E. Springer, C.S. Day, M.W. Wright, S.J. Berners-Price, S.M. Hess, U. Bierbach, *J. Biol. Inorg. Chem.* 9 (2004) 453.

- [15] M.A. Jakupec, M. Galanski, B.K. Keppler, *Reviews of Physiology, Biochemistry and Pharmacology*, Springer-Verlag Berlin, Berlin, 2003.
- [16] M. Galanski, M.A. Jakupec, B.K. Keppler, *Curr. Med. Chem.* 12 (2005) 2075.
- [17] D. Lebowitz, R. Canetta, *Eur. J. Cancer* 34 (1998) 1522.
- [18] R.B. Weiss, M.C. Christian, *Drugs* 46 (1993) 360.
- [19] L.R. Kelland, S.Y. Sharp, C.F. O'Neill, F.I. Raynaud, P.J. Beale, I.R. Judson, *J. Inorg. Biochem.* 77 (1999) 111.
- [20] E. Wong, C.M. Giandomenico, *Chem. Rev.* 99 (1999) 2451.
- [21] A.H. Calvert, S.J. Harland, D.R. Newell, Z.H. Siddik, A.C. Jones, T.J. McElwain, S. Raju, E. Wiltshaw, I.E. Smith, J.M. Baker, M.J. Peckham, K.R. Harrap, *Cancer Chemother. Pharmacol.* 9 (1982) 140.
- [22] Y. Kidani, K. Inagaki, S. Tsukagoshi, *Gann* 67 (1976) 921.
- [23] Y. Kidani, K. Inagaki, M. Ligo, A. Hoshi, K. Kureitani, *J. Med. Chem.* 21 (1978) 1315.
- [24] R.J. Knox, F. Friedlos, D.A. Lydall, J.J. Roberts, *Cancer Res.* 46 (1986) 1972.
- [25] T. Totani, K. Aono, M. Komura, Y. Adachi, *Chem. Lett.* (1986) 429.
- [26] T. Boulikas, M. Vougiouka, *Oncol. Rep.* 10 (2003) 1663.
- [27] K. Itoh, T. Yamashita, H. Wakita, Y. Watanabe, K. Kodama, H. Fujii, H. Minami, T. Ohtsu, T. Igarashi, Y. Sasaki, *Jpn. J. Clin. Oncol.* 28 (1998) 343.
- [28] O. Rixe, W. Ortuzar, M. Alvarez, R. Parker, E. Reed, K. Paull, T. Fojo, *Biochem. Pharmacol.* 52 (1996) 1855.
- [29] S.G. Chaney, A. Vaisman, *J. Inorg. Biochem.* 77 (1999) 71.
- [30] B. Spingler, D.A. Whittington, S.J. Lippard, *Inorg. Chem.* 40 (2001) 5596.
- [31] S.G. Chaney, S.L. Campbell, E. Bassett, Y.B. Wu, *Crit. Rev. Oncol./Hematol.* 53 (2005) 3.
- [32] S.C. Dhara, *Ind. J. Chem.* 8 (1970) 193.
- [33] F.D. Rochon, G. Massarweh, *Inorg. Chim. Acta* 359 (2006) 4095.
- [34] F.D. Rochon, L.M. Gruia, *Inorg. Chim. Acta* 306 (2000) 193.
- [35] P. Bitha, G.O. Morton, T.S. Dunne, E.F. Delossantos, Y.I. Lin, S.R. Boone, R.C. Curtis Haltiwanger, C.G. Pierpont, *Inorg. Chem.* 29 (1990) 645.
- [36] Q.S.L. Ye, Z.Y. Liu, W.P. Liu, S.Q. Hou, X.Z. Chen, *Arch. Pharm. Chem. Life Sci.* 340 (2007) 599.
- [37] T. Mosmann, *J. Immunol. Methods* 65 (1983) 55.
- [38] M.J. Xie, Y. Yu, W.P. Liu, S.Q. Hou, X.Z. Chen, *Acta Crystallogr. Sect. E-Struct. Rep. Online* 63 (2007) M2728.
- [39] M.J. Xie, X.Z. Chen, W.P. Liu, Y. Yu, Q.S. Ye, *Acta Crystallogr. Sect. E-Struct. Rep. Online* 63 (2007) M117.
- [40] B. Beagley, D.W.J. Cruickshank, C.A. McAuliffe, R.G. Pritchard, A.M. Zaki, R.L. Beddoes, R.J. Cernik, O.S. Mills, *J. Mol. Struct.* 130 (1985) 97.
- [41] M.J. Xie, Y. Yu, W.P. Liu, S.Q. Hou, Q.S. Ye, *Acta Crystallogr. Sect. E-Struct. Rep. Online* 63 (2007) M2589.
- [42] S. Neidle, I.M. Ismail, P.J. Sadler, *J. Inorg. Biochem.* 13 (1980) 205.
- [43] F.D. Rochon, R. Melanson, J.P. Macquet, F. Belangergaripey, A.L. Beauchamp, *Inorg. Chim. Acta-Bioinorg. Chem.* 108 (1985) 1.
- [44] K. Sakai, M. Takeshita, Y. Tanaka, T. Ue, M. Yanagisawa, M. Kosaka, T. Tsubomura, M. Ato, T. Nakano, *J. Am. Chem. Soc.* 120 (1998) 11353.
- [45] M.E. Moret, P. Chen, *Eur. J. Inorg. Chem.* (2010) 438.
- [46] G. Cervantes, S. Marchal, M.J. Prieto, J.M. Perez, V.M. Gonzalez, C. Alonso, V. Moreno, *J. Inorg. Biochem.* 77 (1999) 197.
- [47] G.L. Eichhorn, Y.A. Shin, *J. Am. Chem. Soc.* 90 (1968) 7323.
- [48] J. Sambrook, E.F. Fritsche, T. Maniatis, *Molecular Cloning: A Laboratory Manual*, Cold Spring Harbor Press, Cold Spring Harbor, NY, 1989.
- [49] C. Prunkl, M. Pichlmaier, R. Winter, V. Kharlanov, W. Rettig, H.A. Wagenknecht, *Chem.-Eur. J.* 16 (2010) 3392.
- [50] Y.C. Liu, Z.F. Chen, L.M. Liu, Y. Peng, X. Hong, B. Yang, H.G. Liu, H. Liang, C. Orvig, *Dalton Trans.* (2009) 10813.
- [51] A.I. Dragan, E.S. Bishop, R.J. Strouse, J.R. Casas-Finet, M.A. Schenerman, C.D. Geddes, *Chem. Phys. Lett.* 480 (2009) 296.
- [52] J.B. Lepecq, C. Paoletti, *J. Mol. Biol.* 27 (1967) 87.
- [53] J. Olmsted, D.R. Kearns, *Biochemistry* 16 (1977) 3647.